Supporting Information for

Regulating electrode potential offset in perovskite solar cells for boosting interfacial charge transfer

Qiong Wang[1], Mengfan Xue[2], Kaijian Zhu[3], Qiyu Qu[1], Bo Wang[1], Shengyao Wang[4*],

Bing Wang[1], Zhigang Zou[1,5], Wenjun Luo[5*]

[1]Eco-materials and Renewable Energy Research Center (ERERC), Jiangsu Key Laboratory for Nano Technology, National Laboratory of Solid State Microstructures and Department of Physics, Nanjing University, Nanjing 210093, China

[2]Institute of Scientific and Technical Information of China (ISTIC), China

[3]School of Energy and Environment, City University of Hong Kong, 83 Tat Chee Avenue, Kowloon, Hong Kong S.A.R., China

[4]School of Chemistry and Chemical Engineering, Shanghai Jiao Tong University, Shanghai 200240, P. R. China

[5]National Laboratory of Solid State Microstructures, College of Engineering and Applied Sciences, Nanjing University, Nanjing 210093, China

*Email: wjluo@nju.edu.cn; wangshengyao@sjtu.edu.cn

Experimental Methods

Materials

PbI_2 (99.99%), CH_3NH_3I (MAI, 99%), Spiro-TAD (99%), Spiro-TTB (99%), Spiro-OMeTAD (99%), $CF_3SO_2NLiSO_2CF_3$ (Li-TFSI, 99.95%), 4-tert-butylpyridine (TBP, 98%) were purchased from Xi'an Polymer Light Technology. N, N-dimethylformamide (DMF, 99.8%), dimethyl sulfoxide (DMSO, 99.8%), Chlorobenzene (CB, 99.8%), Acetonitrile (ACN, 99.8%), ferrocene (Fc) were purchased from Sigma-Aldrich. The SnO_2 solution was purchased from Alfa Aesar and the I_2 (99.5%) was purchased from Aladdin. Tetrabutylammonium hexafluorophosphate (n-Bu_4NPF_6)) and dichloromethane (DCM, CH_2Cl_2) were purchased from Macklin.

Preparation of samples

The electron transport layer (ETL), perovskite layer and hole transport layer (HTL) were prepared by the spin coating method. The precursor solution of the ETL is prepared by mixing SnO_2 dispersion with deionized water in a volume ratio of 1:5. The 50 μL ETL precursor solution was coated on the FTO substrate for 30 seconds at 3000 rpm, and the prepared film was heated at 180 ℃ for 30 minutes, and then the ETL layer was obtained. The precursor solution of $MAPbI_3$ was prepared by adding 461 mg PbI_2 and 159 mg MAI into the mixed solution of 900 μL DMF and 100 μL DMSO. The precursor solution of 50 μL $MAPbI_3$ was coated on the ETL layer at 4000 rpm for 30 seconds, and at the sixth second of rotation, 150 μL CB was added as the antisolvent, and then the prepared film was heated at 100 ℃ for 10 minutes, and then the perovskite layer was obtained[1]. For the HTL layer, the powder of 72.3 mg Spiro-OMeTAD (or 64.74 mg Spiro-TTB or 58.12 mg Spiro-TAD) was dissolved in 1mL

CB, 17.5 μL Li-TFSI (520 mg Li-TFSI in 1 mL ACN) and 28.8 μL TBP were added. The 50 μL HTL precursor solution was coated on the perovskite layer at 3000 rpm for 30 seconds. And then the film was oxidized in dry air at room temperature for about 36 hours. An Au layer with the thickness of 100 nm was deposited as a top electrode by thermal evaporation.

Characterization of samples

The crystal structure of the samples were measured by X-ray diffractometer (XRD, Rigaku D/MAX-Ultima III, Cu target Kα radiation source). A scanning electron microscope (SEM, Zeiss Gemini 500) was used to observe the morphologies of the samples. The absorption band edges of the samples were obtained by UV-vis absorption spectroscopy (Shimadzu UV 2550). UV photoelectron spectroscopy (UPS, Thermo fisher Esca lab 250Xi, He I hν = 21.22 eV) was used to test the work functions and valence band positions of the samples. Fourier Transform Infrared (FTIR, Shimadzu, IRPrestige-21) spectroscopy was used to measure the chemical bonding of the samples. The schematic diagram of in situ FTIR measurement is shown in Figure S1. In the experiments, the samples were simultaneously illuminated by an AM 1.5 solar simulator and the FTIR source. The FTIR spectra were collected after the samples were illuminated under AM 1.5 solar simulator for different time (0 minutes, 5minutes, 10minutes, 15 minutes and so on).

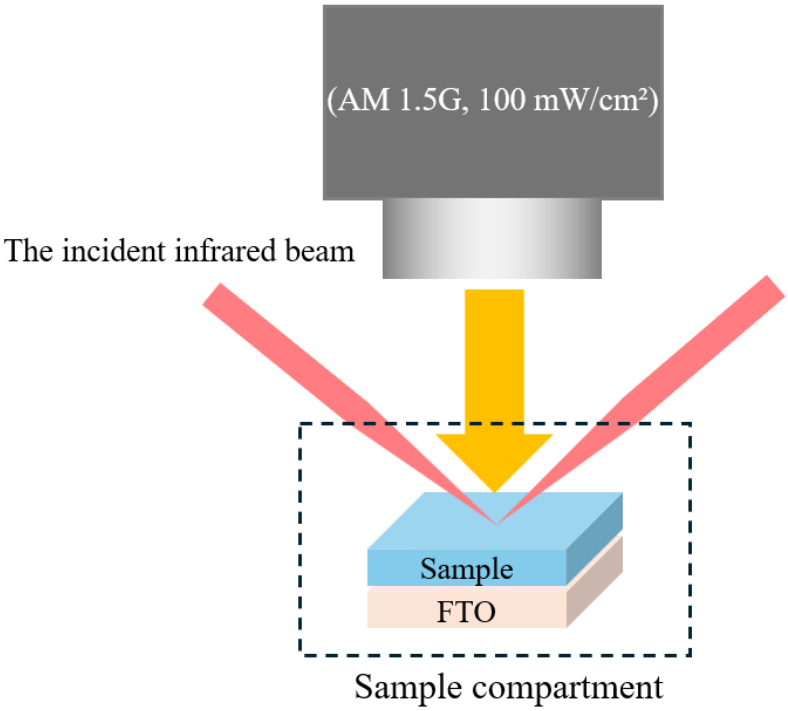

Figure S1. Schematic diagram of in-situ infrared measurement.

The molecular structures of the samples characterized by NMR spectroscopy (Bruker 600' 54 Ascend LH 600MHz)[2]. The surface morphology and roughness of the sample were characterized by atomic force microscopy (AFM) which were performed using a Dimension Icon instrument (Bruker, USA). The hole mobilities of the HTLs were measured by space charge limited current (SCLC) and current density-voltage (J-V) characteristics were recorded by a source (Keithley 2400). The electrical conductivity of the samples was performed using the four-point probe method (RTS-9 dual-configuration four-point probe measurement system)

Theoretical Calculations

Theoretical calculations were performed using Gaussian software. Molecular configurations were optimized at the B3LYP-D3 (BJ)/def2-TZVP level of theory[3-4]. Models were established for three HTLs and their iodinated derivatives (with hydrogen at the side chain positions replaced by I_2), as well as for I_2 and hydrogen iodide (HI). The reaction as follow: HTL + I_2 →

HTL-I + HI, where HTL-I represents the iodinated derivative of HTL. Gibbs free energy changes of these reactions were calculated.

Electrochemical measurements

The electrochemical tests in this study were carried out in a standard three-electrode system. The electrochemical analyzer was a Shanghai Chenhua CHI760e (Shanghai Chenhua). The electrolyte was 0.1M n-Bu_4NPF_6 in CH_2Cl_2 solution, the sample was the working electrode, a metal Pt wire was a counter electrode, an Ag wire electrode was used as a pseudo-reference electrode. All of the potentials relative to the Ag electrode were converted to potentials relative to ferrocene (Fc), by adding 1 mM ferrocene to the electrolyte and measuring the reaction potential of ferrocene through a Pt wire. Using ferrocene as an internal standard, the potential at which this redox pair (Fc/Fc^+) occurs was specified as 0 V vs. Fc/Fc^+. The vacuum energy level of Fc/Fc^+ is -4.9 eV.

Photovoltaic measurements

The photovoltaic performance were measured in a nitrogen-filled glovebox, with the light intensity calibrated to one standard sun (Enlitech, AM 1.5G, 100 mW/cm²). J-V characteristics were recorded by a source (Keithley 2400). The device structure used in the SCLC test was FTO/PEDOT:PSS/HTL/Au.

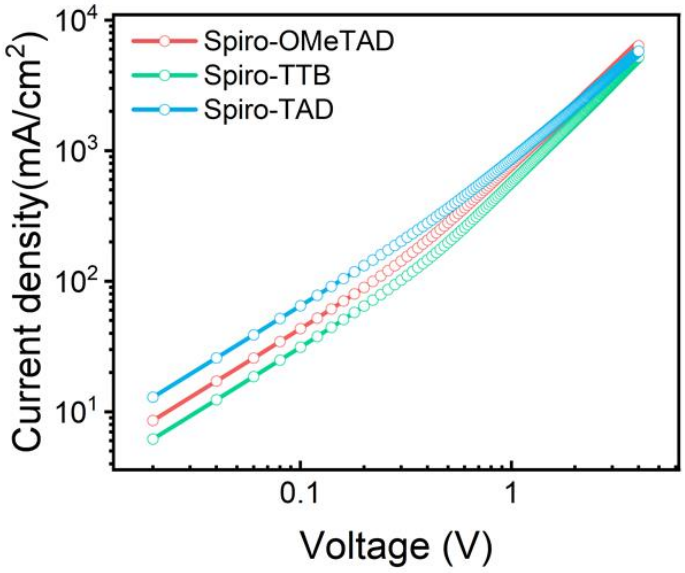

Figure S2. J-V curves of the hole-only devices with an architecture of FTO/PEDOT:PSS/HTL/Au.

Table S1: Th values of hole mobility and conductivity of three HTLs.

HTL Name	Hole mobility (cm^2 / V·s)	Film conductivity (S/cm)
Spiro-OMeTAD	8.10E-3	7.35E-5
Spiro-TTB	6.96E-3	5.76E-5
Spiro-TAD	6.56E-3	4.68E-5

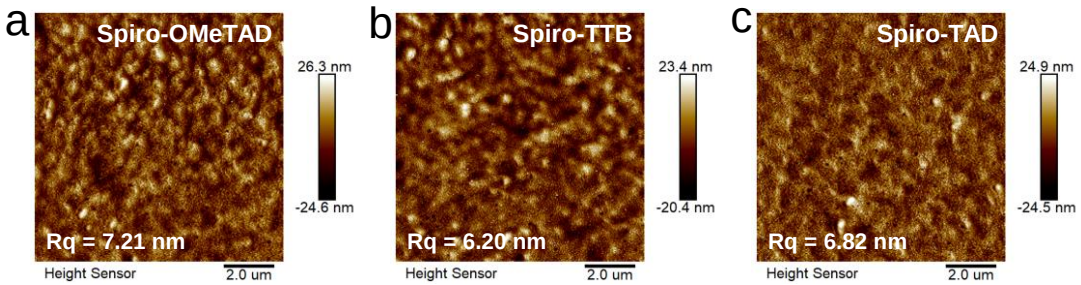

Figure S3. The AFM images of (a) Spiro-OMeTAD, (b) Spiro-TTB, (c) Spiro-TAD.

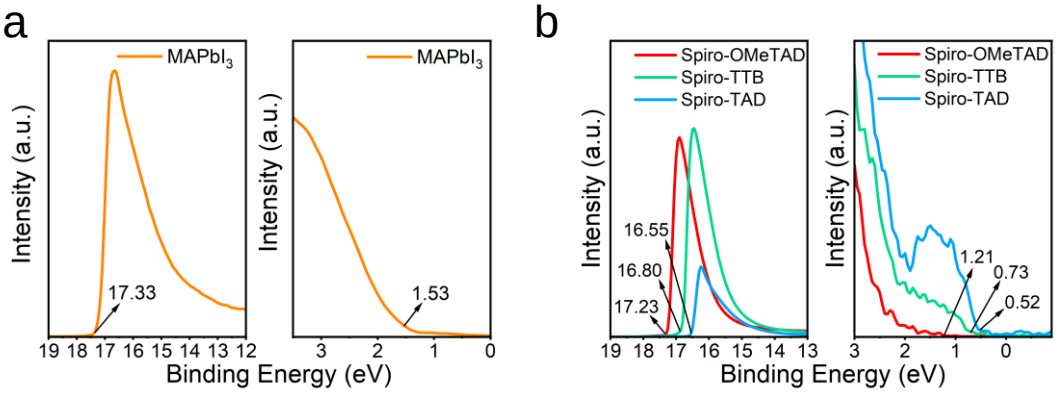

Figure S4. UPS spectra of (a) $MAPbI_3$ and (b) three HTLs.

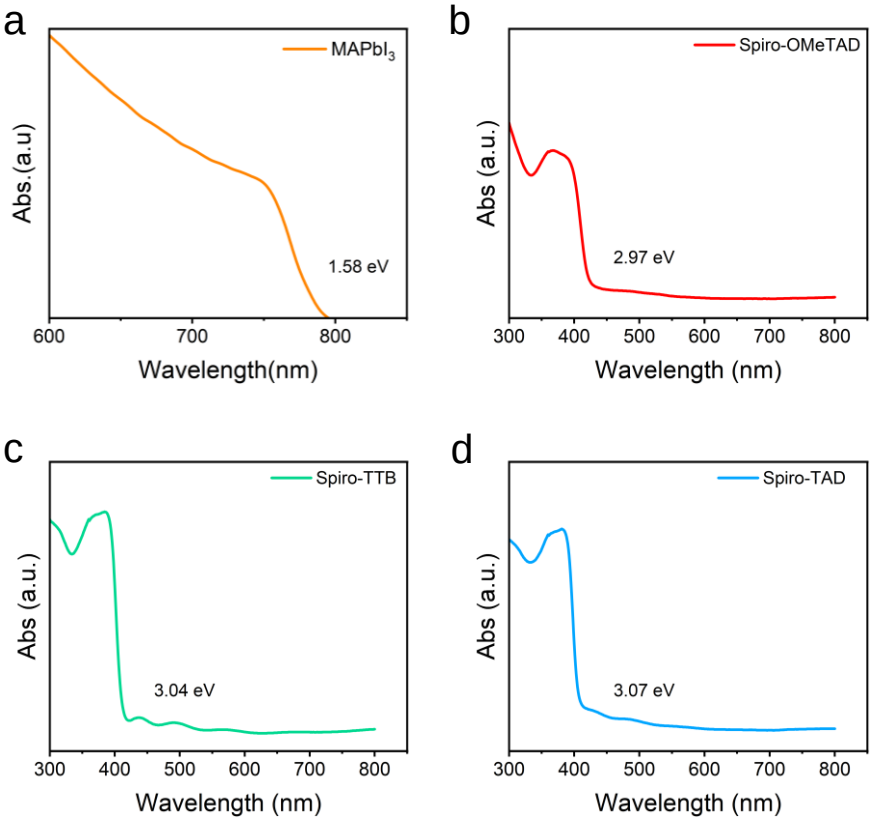

Figure S5. UV-vis spectra of (a) $MAPbI_3$, (b)Spiro-OMeTAD, (c)Spiro-TTB, (d)Spiro-TAD.

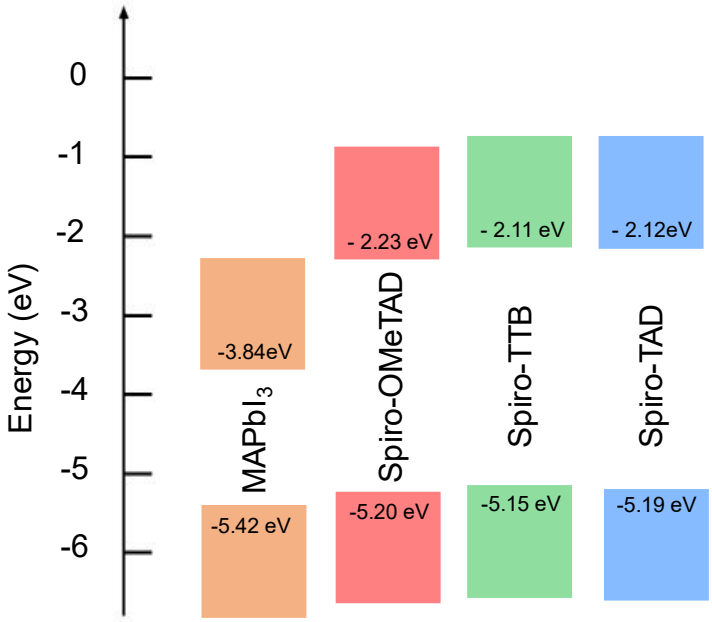

Figure S6. Conduction and valence band position of $MAPbI_3$ and the HOMO and LUMO levels of three kinds of HTLs.

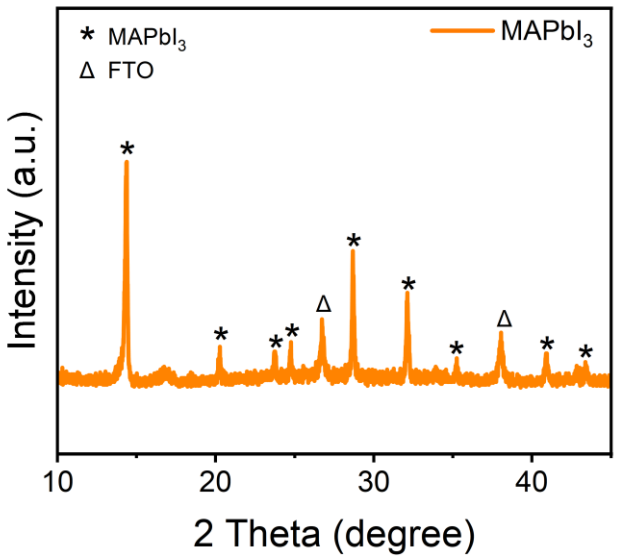

Figure S7. XRD pattern of $MAPbI_3$.

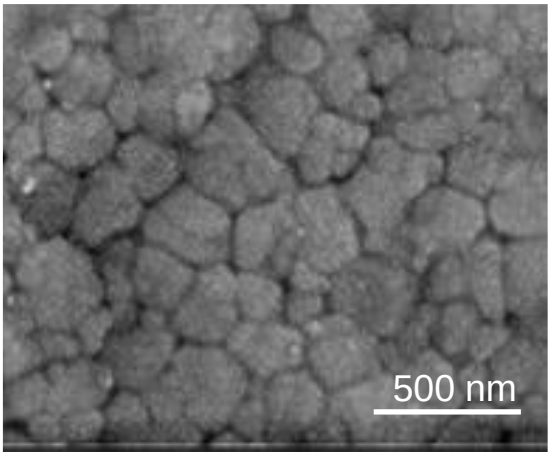

Figure S8. SEM image of $MAPbI_3$.

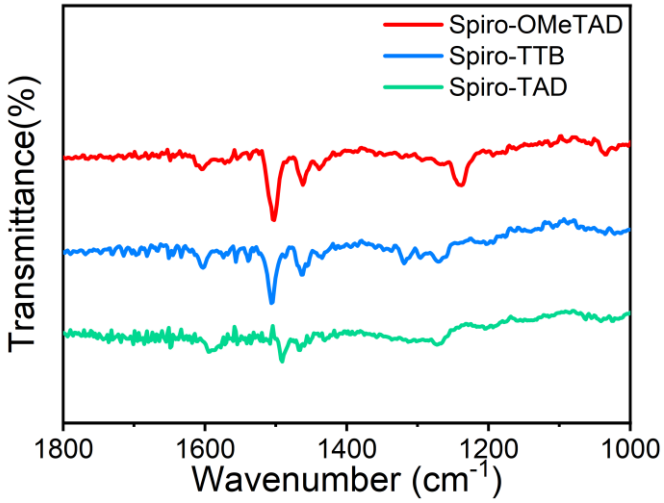

Figure S9. FTIR of three HTLs.

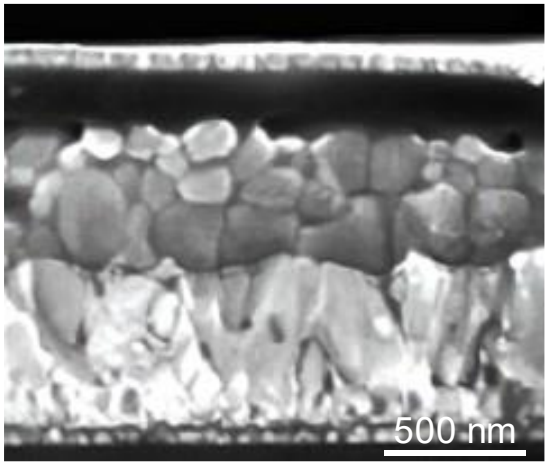

Figure S10. SEM cross-sectional images of FTO/SnO_2/$MAPbI_3$/Spiro-OMeTAD/Au.

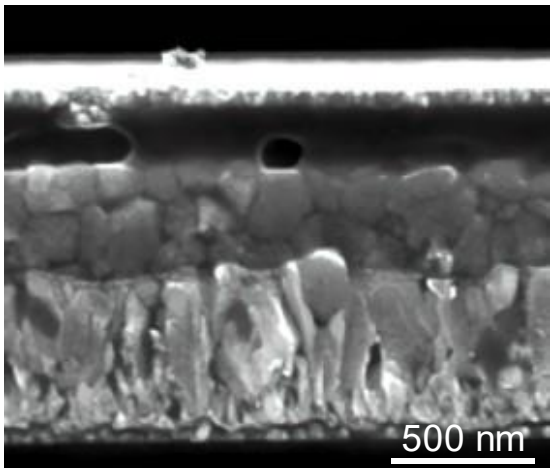

Figure S11. SEM cross-sectional images of FTO/SnO_2/$MAPbI_3$/Spiro-TTB/Au.

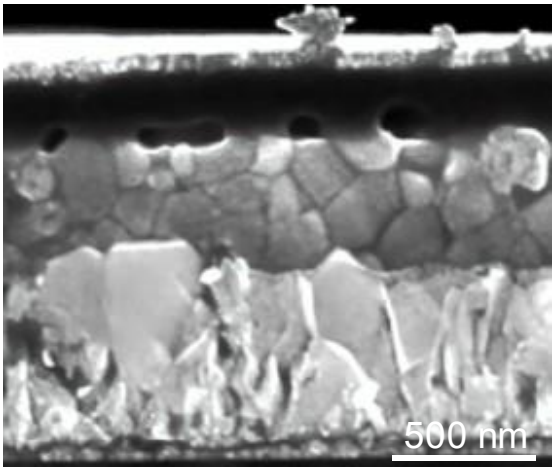

Figure S12. SEM cross-sectional images of FTO/SnO_2/$MAPbI_3$/Spiro-TAD/Au.

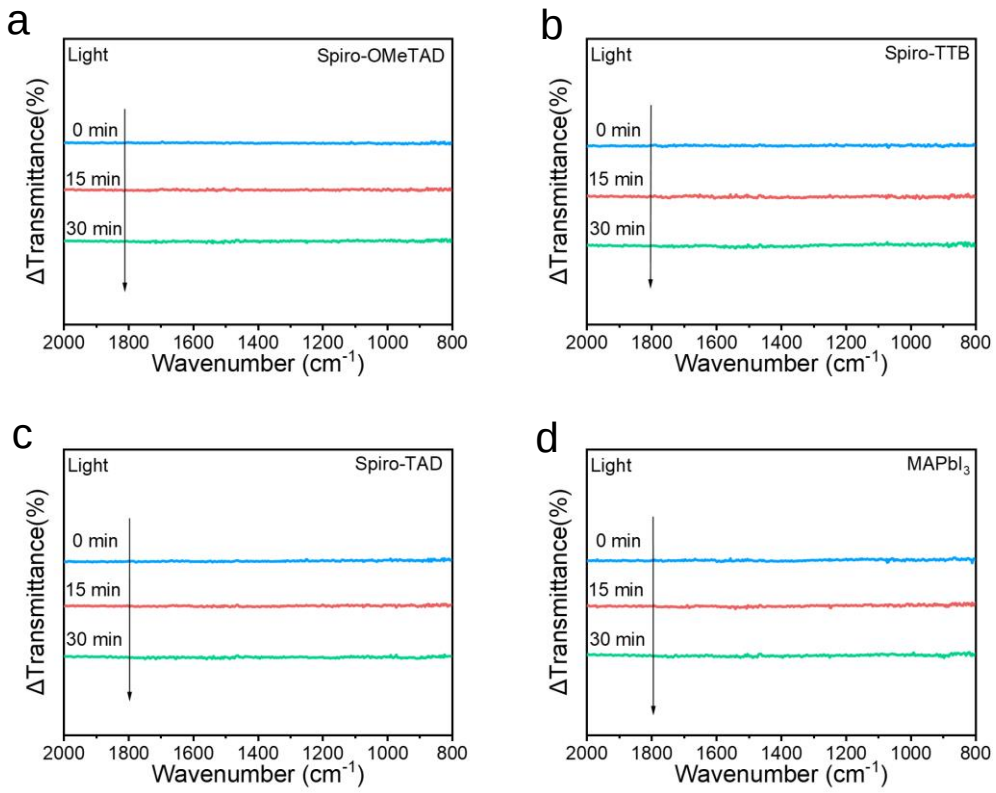

Figure S13. In situ FTIR of single material under illumination. (a) Spiro-OMeTAD, (b) Spiro-TTB, (c) Spiro-TAD and (d) $MAPbI_3$.

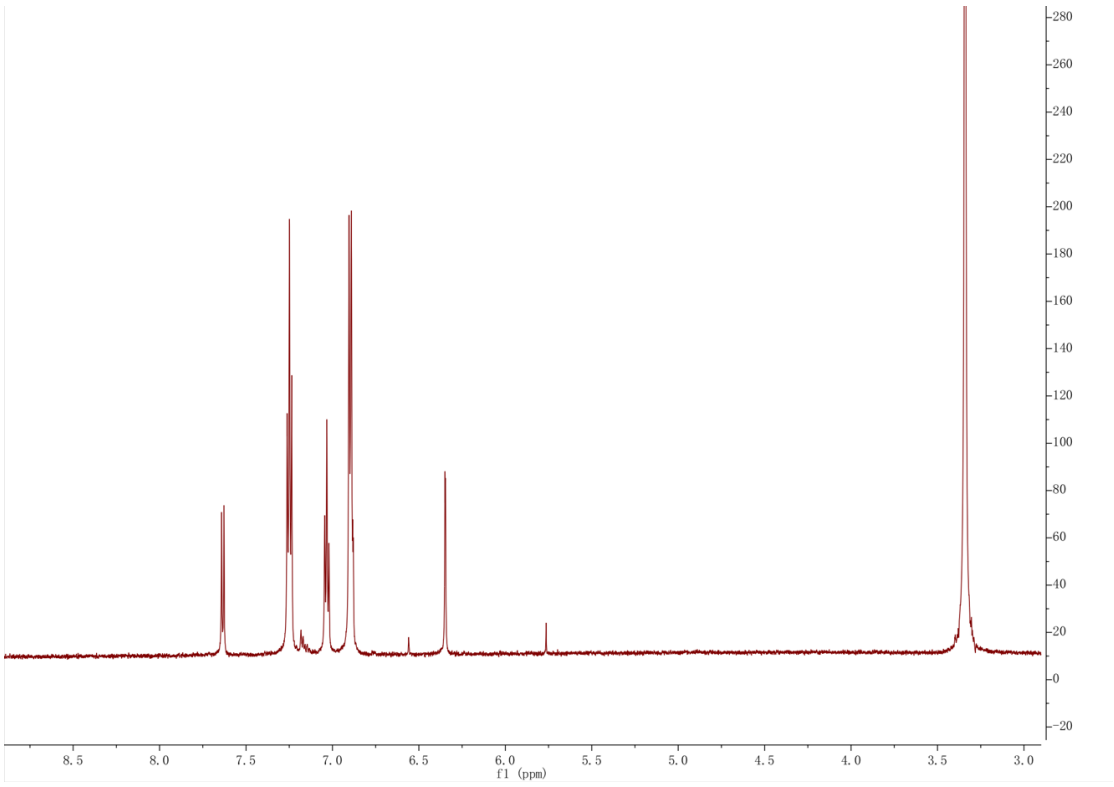

Figure S14. ^1H NMR spectra of Spiro-TAD powder.

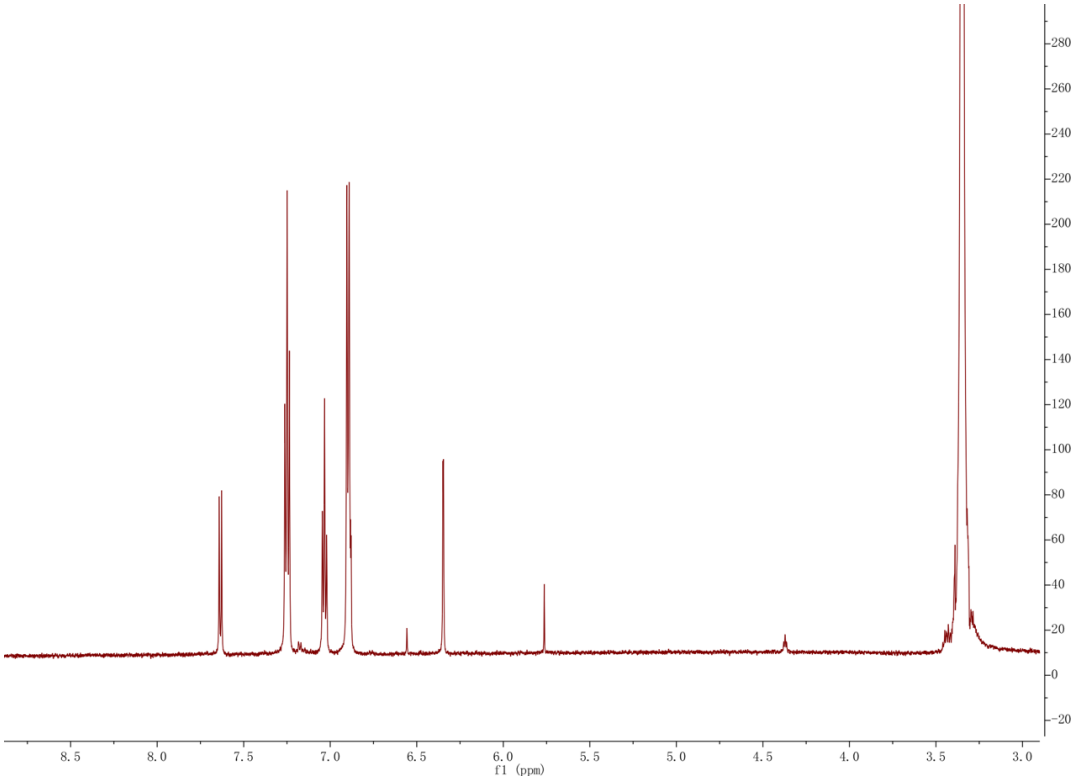

Figure S15. ^{1}H NMR spectra of Spiro-TAD powder after exposure to I_2 vapor for 10 minutes in the dark.

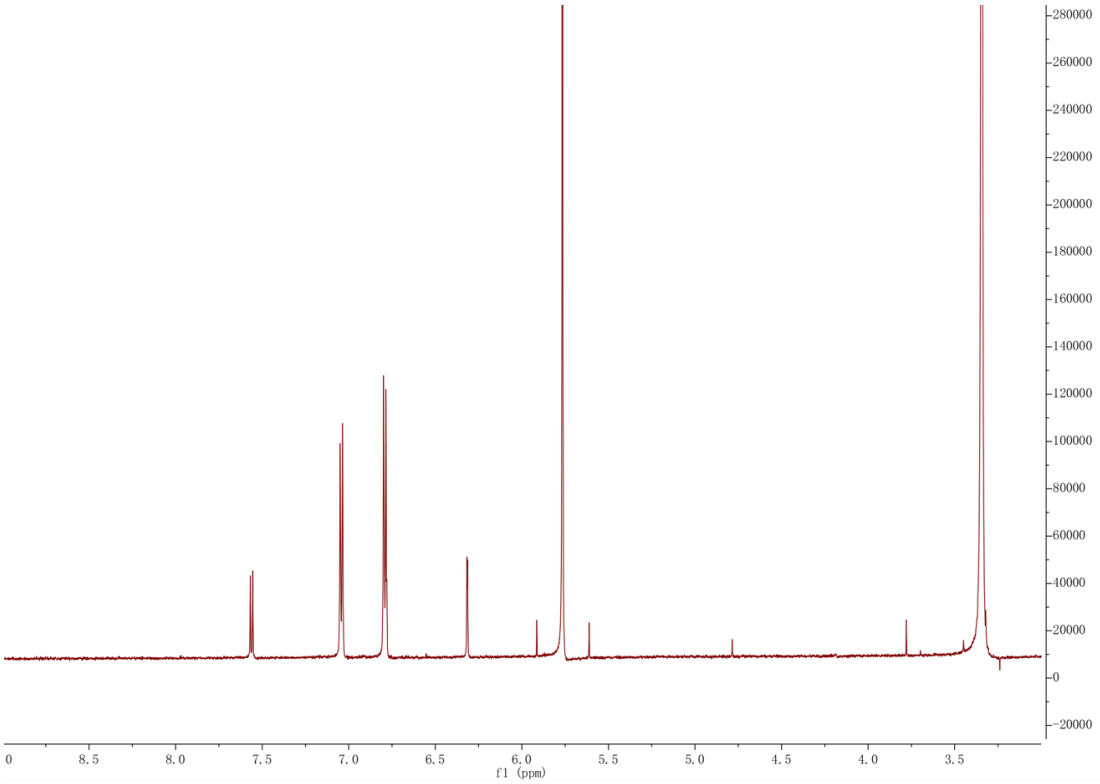

Figure S16. ^{1}H NMR spectra of Spiro-TTB powder.

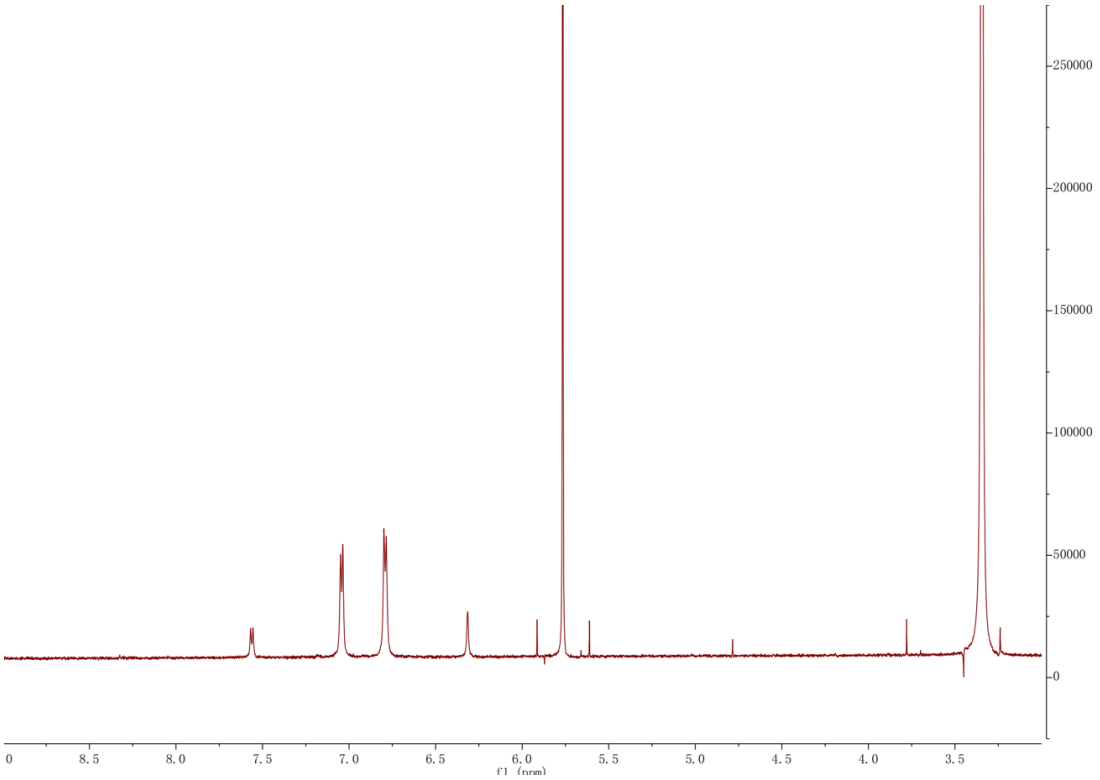

Figure S17. ^{1}H NMR spectra of Spiro-TTB powder after exposure to I_2 vapor for 10 minutes in the dark.

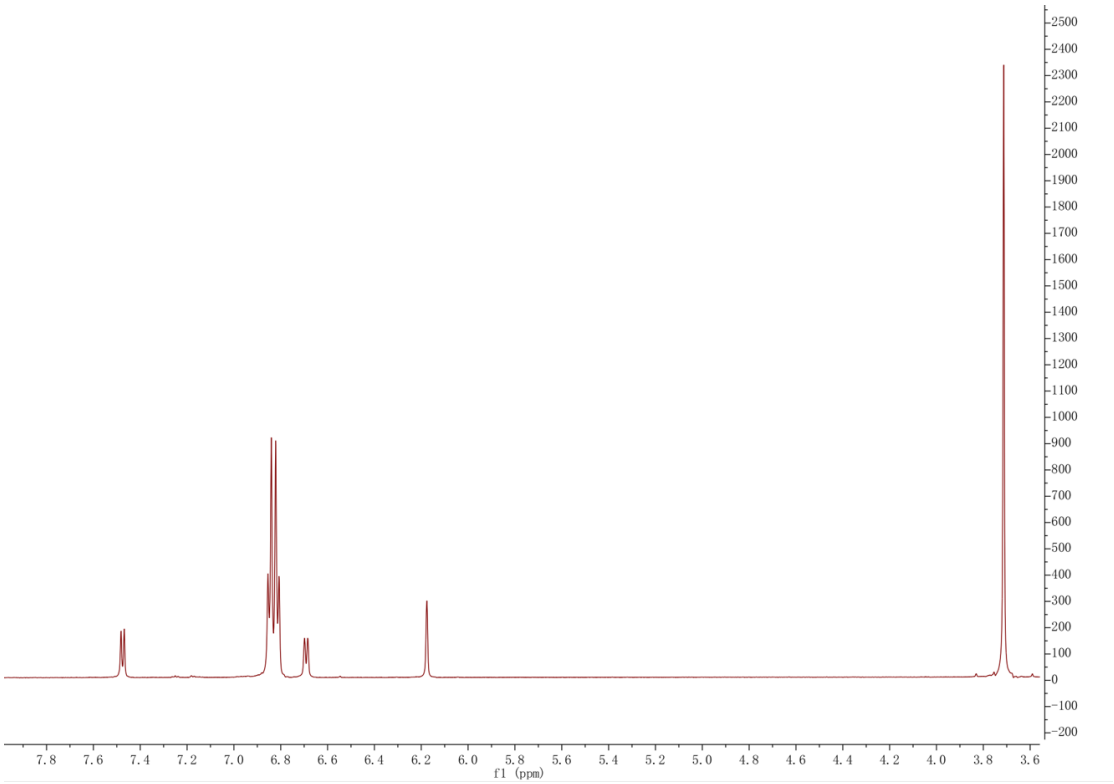

Figure S18. ^{1}H NMR spectra of Spiro-OMeTAD powder.

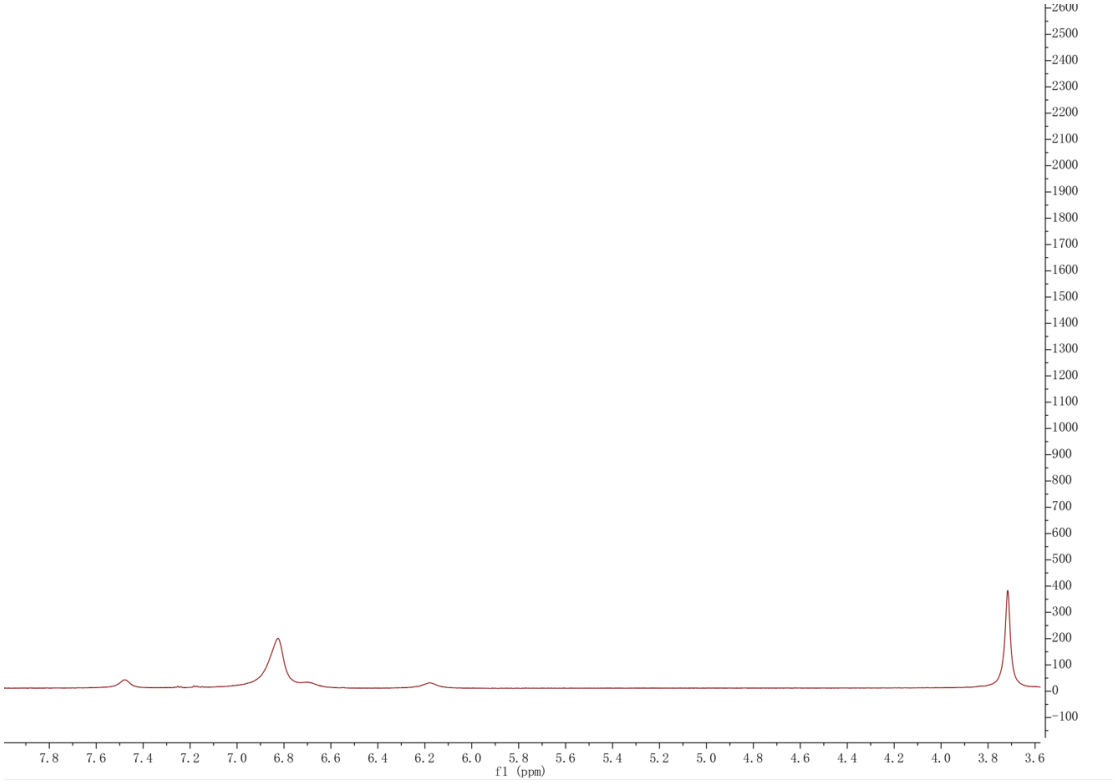

Figure S19. ^{1}H NMR spectra of Spiro-OMeTAD powder after exposure to I_2 vapor for 10 minutes in the dark.

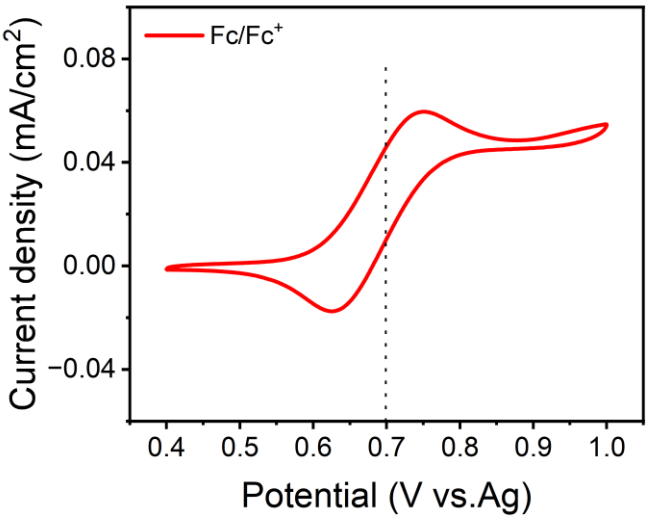

Figure S20. Cyclic voltammetry (CV) curve of Pt wire in the electrolyte of 1 mM ferrocene and 0.1 M n-Bu_4NPF_6 in CH_2Cl_2 (N_2)[5].

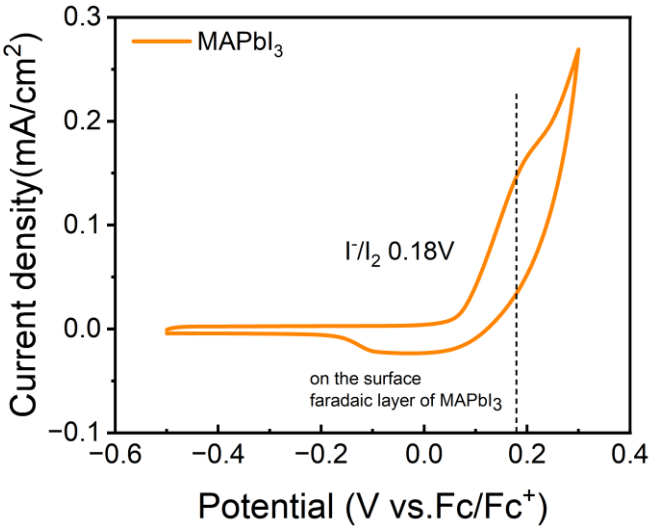

Figure S21. CV curve of $MAPbI_3$ in the dark. (0.1 M n-Bu_4NPF_6 in CH_2Cl_2, N_2)[5].

References

1. Cao, Y.; Liu, Z.; Li, W.; Zhao, Z.; Xiao, Z.; Lei, B.; Zi, W.; Cheng, N.; Liu, J.; Tu, Y. Efficient and Stable $MAPbI_3$ Perovskite Solar Cells Achieved via Chlorobenzene/Perylene Mixed Anti-Solvent. Solar Energy., 2021, *220*, 251–257.
2. Zhang, T.; Wang, F.; Kim, H.-B.; Choi, I.-W.; Wang, C.; Cho, E.; Konefal, R.; Puttisong, Y.; Terado, K.; Kobera, L.; Chen, M.; Yang, M.; Bai, S.; Yang, B.; Suo, J.; Yang, S.-C.; Liu, X.; Fu, F.; Yoshida, H.; Chen, W. M.; Brus, J.; Coropceanu, V.; Hagfeldt, A.; Brédas, J.-L.; Fahlman, M.; Kim, D. S.; Hu, Z.; Gao, F. Ion-Modulated Radical Doping of Spiro-OMeTAD for More Efficient and Stable Perovskite Solar Cells. Science., 2022, *377* (6605), 495–501.
3. Hu, S.; Li, T.; Huang, M.; Huang, J.; Li, W.; Wang, L.; Chen, Z.; Fu, Z.; Li, X.; Liang, Z. Phenylene-Bridged Bispyridinium with High Capacity and Stability for Aqueous Flow Batteries. Adv. Mater., 2021, 33 (7), 2005839.
4. Zhang, Q.; Zhao, Q.; Wang, H.; Yao, Y.; Li, L.; Wei, Y.; Xu, R.; Zhang, C.; Shalenov, E. O.; Tu, Y.; Wang, K.; Xiao, M. Tuning Isomerism Effect in Organic Bulk Additives Enables Efficient and Stable Perovskite Solar Cells. Nano-Micro Lett., 2025, *17* (1), 107.
5. Cardona, C. M.; Li, W.; Kaifer, A. E.; Stockdale, D.; Bazan, G. C. Electrochemical

Considerations for Determining Absolute Frontier Orbital Energy Levels of Conjugated Polymers for Solar Cell Applications. Adv. Mater., 2011, 23 (20), 2367–2371.

6. Xue, M.; Li, Z.; Wang, Q.; Chen, Y.; Luo, J.; Bao, R.; Jiang, D.; Wang, S.; Wang, B.; Yu, T.; Yao, Y.; Luo, W.; Zou, Z. Origin of V_{OC} in Perovskite Solar Cells by Faradaic Junction Model. Sci. China Chem., 2025, 2025-10-20. DOI: /10.1007/s11426-025-3073-0.